

# Biomolecular Fishing for Calixarene Partners by a Chemoproteomic Approach

Stefano Tommasone, Carmen Talotta, Carmine Gaeta,\* Luigi Margarucci, Maria Chiara Monti, Agostino Casapullo,\* Beatrice Macchi, Salvatore Pasquale Prete, Adriana Ladeira De Araujo, and Placido Neri\*

**Abstract:** MS-based chemical-proteomics technology is introduced herein as a third general strategy to study the biomolecular recognition properties of given calixarene derivatives. In particular, we demonstrate that a simply designed calix[4]arene derivative **1a** bearing acetamido groups at the *exo* rim (pAC), when linked to a solid support, is able to fish out a specific protein (PDI protein) from a crude extract of HeLa cells. Western blot and surface plasmon resonance studies confirmed the direct interaction between PDI and the linker-free pAC derivative **1b** with considerable affinity, and *in vitro* tests showed its inhibition of PDI chaperone activity. In accordance with the role of PDI in a variety of human cancers, biological tests showed that pAC **1b** was cytotoxic and cytostatic toward CAL-27 and PC-3 cancer cell lines *in vitro*. Docking studies showed that H bonds and hydrophobic interactions contribute to the stabilization of the PDI/pAC complex.

In the past two decades, a considerable amount of attention has been devoted to biomolecular recognition by calixarene derivatives and in particular to their interaction with drugable targets.<sup>[1]</sup> In this regard, calixarene derivatives able to selectively bind a known biomolecular target have been identified through two principal strategies: experimental screening of a library of calixarene derivatives<sup>[1c,d,j]</sup> or virtual screening with molecular docking.<sup>[1h,k,m]</sup>

Regarding the first strategy, in a pioneering study, Hamilton and co-workers<sup>[1c]</sup> synthesized a library of peptidocalixarenes, from which they identified a diversomer able to

selectively bind to PDGF growth factor, thus resulting in significant inhibition of tumor growth and angiogenesis *in vivo*. Interestingly, their results also showed a lack of toxicity of the calixarene framework in several *in vivo* biological tests. Analogous observations were reported by Liu and co-workers,<sup>[2a]</sup> who proved that *p*-sulfonatocalix[*n*]arenes showed no toxic effects in mice poisoned with viologen derivatives; instead, the mortality rate of the mice was significantly decreased. Coleman et al. demonstrated that, in mice, a single injection of a calix[4]arene derivative, at doses equivalent to 2–5 g in humans, showed no acute toxicity, and the compound was rapidly cleared by elimination in urine without accumulating in the liver.<sup>[2b]</sup> All these results have prompted many researchers to pursue the discovery of new calixarene hosts able to recognize biomolecular targets. In this vein, we reported the synthesis of a series of peptidocalixarene diversomers, a few of which were able to inhibit transglutaminase enzymes by surface recognition.<sup>[1i]</sup>

Regarding the second strategy, the identification of bioactive calixarene derivatives by molecular docking has been attracting more and more interest, since it offers insight into the secondary interactions involved in the stabilization of the protein–ligand complex. Thus, de Mendoza and co-workers reported the computer-assisted design of a tetramethylguanidium calix[4]arene derivative,<sup>[1k]</sup> which was able to recognize the tetrameric protein p53TD-R337H mutant by a combination of hydrophobic interactions, ion pairing, and hydrogen bonding. We designed arylamido calix[4]arene derivatives as effective histone deacetylase inhibitors (HDACis) by molecular-docking screening.<sup>[1h]</sup> In particular, molecular-docking studies provided evidence that the van der Waals interactions between the large hydrophobic groups at the *exo* rim of the calixarene derivatives and the four external hydrophobic pockets on the enzyme surface are essential for the stabilization of the HDAC–calixarene complex.

The development of novel strategies to identify possible biological targets for given calixarene derivatives is crucial for understanding of their biomolecular recognition abilities. Nowadays, remarkable advances in analytical methods, and in particular in chemical-proteomics technologies based on mass spectrometry, have a marked impact on target discovery. One of the major chemical-proteomics approaches employs immobilized compounds that can be used for affinity enrichment of their interacting targets in samples from cells and tissues.<sup>[3]</sup>

We envisioned that such a chemical-proteomics approach could be used as a third general strategy to study the biomolecular-recognition abilities of a given calixarene deriv-

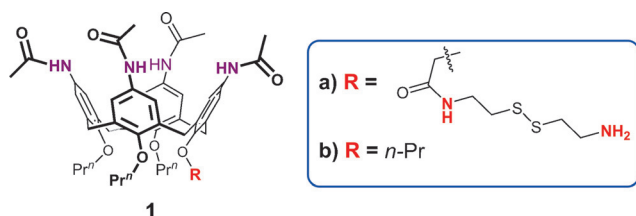
[\*] Dr. S. Tommasone, Dr. C. Talotta, Prof. C. Gaeta, Prof. P. Neri  
Dipartimento di Chimica e Biologia “A. Zambelli”  
Università di Salerno  
Via Giovanni Paolo II 132, 84084 Fisciano (Salerno, Italy)  
E-mail: cgaeta@unisa.it  
neri@unisa.it

L. Margarucci, Dr. M. C. Monti, Prof. A. Casapullo  
Dipartimento di Farmacia, Università di Salerno  
Via Giovanni Paolo II 132, 84084 Fisciano (Salerno, Italy)  
E-mail: casapullo@unisa.it

Dr. B. Macchi, Dr. S. P. Prete  
Dipartimento di Medicina dei Sistemi  
Università di Roma Tor Vergata  
Via Montpellier 1, 00133 Roma (Italy)

Dr. A. Ladeira De Araujo  
Department of Pathology, Laboratory of Dermatology and Immunodeficiencies, Medical School, University of Sao Paulo (Brasil)

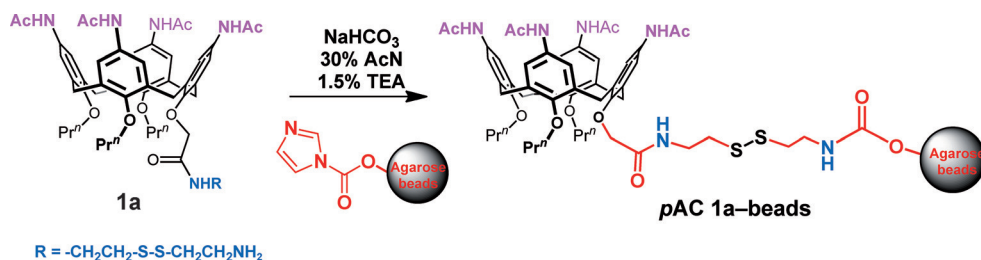
Supporting information for this article is available on the WWW under <http://dx.doi.org/10.1002/ange.201508651>.



Scheme 1. Structure of *p*-acetamidocalix[4]arenes (*p*ACs) **1a,b**.

ative. In particular, the *p*-acetamidocalix[4]arene (*p*AC) derivative **1a** (Scheme 1) combines the hydrogen-bond-donor/acceptor abilities of the acetamido groups<sup>[4]</sup> and the hydrophobicity of the calixarene backbone, and both factors should favor the formation of novel protein–calixarene complexes.<sup>[1h,k]</sup> Our experimental procedure consisted of the following steps: 1) synthesis of *p*-acetamidocalix[4]arene (*p*AC) derivatives; 2) chemical immobilization of the *p*ACs on a solid support; 3) incubation of the *p*AC-modified beads with cell lysates; 4) identification of species interacting with the *p*ACs by mass spectrometry; 5) evaluation of the bioactivity of the *p*ACs by in vitro and in-cell assays.

We designed the derivative **1a** to have a suitable spacer arm at the *endo* rim, 2-(2-aminoethylthio)ethylamine (TIOS), for immobilization onto an agarose CDI matrix (solid support). Such a spacer is usually required to minimize steric hindrance between the ligand on the matrix and its macromolecular partners during the affinity-purification step.<sup>[5]</sup> Derivative **1a** was synthesized (see Scheme S1 in the Supporting Information), purified by HPLC, and characterized by <sup>1</sup>H and <sup>13</sup>C NMR spectroscopy and ESI(+) MS.<sup>[6]</sup> It was then linked covalently through its free amino group to solid beads made of CDI agarose activated with 1,1'-carbonyldiimidazole (Scheme 2).<sup>[6]</sup> The experimental conditions (buffer,



Scheme 2. Immobilization of *p*AC derivative **1a** on agarose beads. TEA=triethylamine.

pH value, incubation time, and temperature) were optimized for the preparation of beads with a final **1a** concentration of 3 μmol per milliliter of resin, and the coupling process was monitored by reversed-phase HPLC analysis (see Figure S3 in the Supporting Information).<sup>[6]</sup>

Samples of crude HeLa cell extracts were incubated with *p*AC **1a** on the solid support and with the *p*AC-free matrix as a control experiment to discern between specific and aspecific interactions. After extensive washing, the beads were treated with dithiothreitol (DTT) to break the disulfide bridge on the linker and to release into solution the proteins strictly bound to the *p*AC derivative (Figure 1). The protein mixtures were

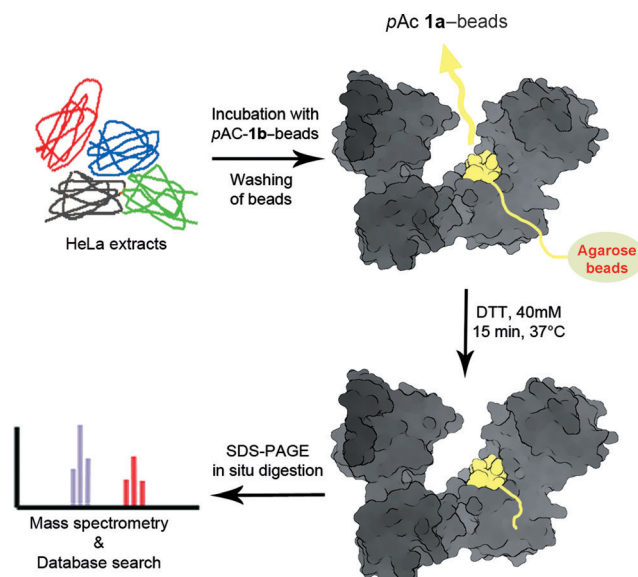


Figure 1. Schematic illustration of the approach of biomolecular fishing with *p*AC **1a**-beads.

then purified by SDS-PAGE (see Figure S6); the entire gel was cut, digested with trypsin, and analyzed by mass spectrometry through nanoflow reversed-phase HPLC MS/MS (Figure 1; see also Figure S7).<sup>[6]</sup> Doubly and triply charged peptide species were fragmented, and all the MS/MS spectra were subjected to a Mascot database search (see Figures S9–S11).<sup>[6]</sup> The identified proteins were then compared with those of the free-matrix control experiment (see Table S2), and those present in both experiments were excluded to give a set of potential protein partners (see Table S1). As is usual for this kind of pulldown experiment,<sup>[3,5]</sup>

a large number of potential partners was found in the raw data. This number was strongly reduced by applying a filter on the Mascot scores and the individual Pep(sig) values, thus giving a lower, reasonable number of molecules that were potentially interacting with the *p*AC.

To establish which protein was the best potential partner, the entire fishing/control procedure was repeated twice to give three sets of potential partners (see Tables S1 and S3). The intersection of these sets was identified to exclude all noncommon candidates (see Table S4). In this way, a single protein common to the three sets was found (Figure S8). This protein, protein disulfide isomerase (PDI), was considered as the best potential partner of *p*AC **1a**.<sup>[7]</sup> PDI is a 57 kDa chaperone protein located in the endoplasmic reticulum (ER).<sup>[8,9]</sup> Acting as a thiol oxidoreductase, PDI catalyzes the formation, breakage, and rearrangement of disulfide bonds, and therefore regulates oxidative protein folding as well as cell viability.<sup>[10]</sup> Located in the two PDI active sites, in the **a** and

**a'** domains, are two conserved cysteine residues, which are essential for PDI activity and for the cycle between the oxidized (disulfide) and reduced (dithiol) state.<sup>[11]</sup> Increased PDI levels have been documented in a variety of human cancers, including ovarian,<sup>[12]</sup> prostate,<sup>[13]</sup> and lung cancers,<sup>[14]</sup> as well as lymphoma,<sup>[15]</sup> glioma,<sup>[16]</sup> and acute myeloid leukemia.<sup>[17]</sup> Inhibition of PDI activity leads to apoptosis in cancer,<sup>[10a]</sup> thus suggesting that PDI is a promising druggable target.

To verify whether the disulfide bridge of **1a** may have a role in the interaction with PDI protein, we studied the interaction of **1a** and of the sulfur-free derivative **1b**, bearing four propyl chains at the lower rim, with PDI protein through western blot and surface plasmon resonance (SPR) methods.<sup>[6]</sup> Western blot results clearly indicated that **1b** was able to bind PDI protein, thus demonstrating that the interaction between **1a** and PDI protein does not occur through the disulfide bridge (see Figure S12).<sup>[6]</sup> SPR analysis was performed by immobilizing PDI on the surface of a CM5 chip, and then injecting solutions of *p*AC **1b** (at three different concentrations, 0.1–10  $\mu\text{M}$ ) to give the association and dissociation curves. The results (see Figure S13) clearly showed a considerable affinity ( $K_D = 11 \mu\text{M}$ )<sup>[6]</sup> between the PDI/**1b** counterparts, thus confirming their direct interaction. To confirm the specificity of the interaction, *p*AC **1b** was injected over two different proteins (peroxiredoxin 1 and Laminin B1) as negative controls, as well as over the unfunctionalized SPR chip; in these experiments, no binding was observed (see Figures S14–S16).<sup>[6]</sup>

We performed a molecular-docking study to confirm and rationalize the observed biological results and to gain more insight into the interaction of *p*AC **1b** with PDI (Figure 2). Protein disulfide isomerase features four thioredoxin domains, **a**, **b**, **b'**, and **a'** (Figure 2a),<sup>[18]</sup> arranged in the shape of a twisted “U”. The two active sites are located in the **a** and **a'** domains and face each other across the long sides of the “U”. They are separated by 28 Å, as measured between the S atoms of catalytically active cysteine residues. The **b'** domain contains a large hydrophobic pocket able to accommodate the substrate (Figure 2a).<sup>[18]</sup> The inside surface of the “U” is enriched in hydrophobic residues, thereby facilitating interactions with misfolded proteins. In fact, a solid-state

study<sup>[15]</sup> showed that these hydrophobic residues are crucial for the interaction between PDI and its substrates, which are either unfolded or partially folded proteins containing exposed hydrophobic residues.

Our docking studies showed that *p*AC **1b** occupied the inside surface of the “U”, and was deeply bound in the hydrophobic pocket in the **b'** domain (Figure 2a; see also Figure S19), a region essential for interactions with hydrophobic protein substrates.<sup>[18b]</sup> A close inspection of the preferred binding site revealed that **1b** established two hydrogen bonds with Trp396 and His438 (Figure 2b; see also Figure S20a), and a  $\pi$ -stacking interaction was identified between an aromatic ring of **1b** and Phe249 (see Figures S20 and S21). Furthermore, van der Waals interactions were established between the hydrophobic walls of **1b** and the apolar lateral chains of Ile, Phe, and Leu amino acid residues in the PDI binding site (see Figure S18). A recent report by Wang and co-workers<sup>[18b]</sup> showed that Trp396, a highly conserved residue located in the immediate proximity of the active site containing Cys397, plays an essential role in the redox-regulated conformational change between reduced and oxidized PDI forms. Interestingly, this conformational change between the different redox states of PDI directly modulates the chaperone activity of PDI protein.<sup>[18b]</sup> The studies of Wang and co-workers showed that in the reduced form of PDI, Trp396 forms a cation– $\pi$  interaction with Arg300, and that this interaction is broken upon the oxidation of PDI.<sup>[18b]</sup> Interestingly, Wang and co-workers demonstrated that the mutation of Trp396 significantly impairs<sup>[19]</sup> the redox-regulated conformational change of PDI. These observations led us to conclude that the hydrogen-bonding interactions between *p*AC **1b** and Trp396 would interfere with the conformational change between reduced and oxidized PDI forms that is essential for the catalytic activity of the enzyme. Furthermore, as evidenced by docking results, the occupation of the PDI hydrophobic pocket **b'** by *p*AC **1b** through van der Waals interactions could hinder the binding of substrates.

Interestingly, docking calculations revealed an inhibition constant,  $K_i = 6.23 \mu\text{M}$  (see Table S4), very similar to that obtained by SPR analysis ( $K_D = 11 \mu\text{M}$ ). To verify the accessibility of the enzyme active site, without disruption of the PDI complex, to beads modified with *p*AC **1a**, as required by the fishing experiments, we performed a molecular-docking study with a linker-bearing model compound (see Figure S18). Also in this case, the calixarene unit bound the PDI in the same pocket of **1b** with similar H-bonding and van der Waals interactions (see Figures S22 and S23). In a similar way, molecular docking confirmed the crucial role of the acetamido groups of **1b**. In fact, its *p*-tert-butyl analogue clearly showed poor affinity for the PDI protein ( $K_i = 8.23 \text{ mM}$ ; see Figures S18 and S24).

At this point, we moved to the analysis of the biological profile of *p*AC **1b**, and first investigated its potential modulation of the PDI activity. Since PDI plays a key role in protein folding by catalyzing the rearrangement of disulfide bonds in substrate proteins, we performed an *in vitro* test based on the enzyme-catalyzed reduction of insulin (see Figure S17) and spectrophotometric measurement of the aggregation of reduced insulin chains.<sup>[20]</sup> In this method,

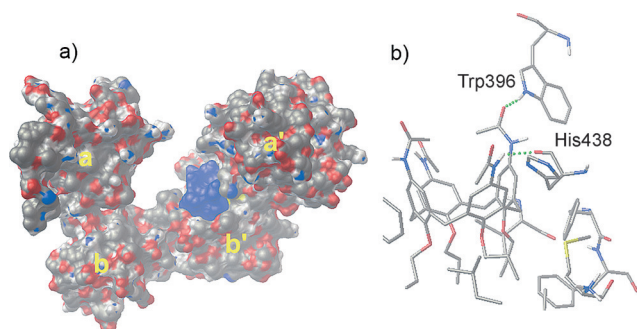


**Figure 2.** Docking experiments. a) 3D model of the binding mode of *p*AC **1b** in the hydrophobic pocket in the **b'** domain of PDI. The protein molecular surface is shown (colored according to atom type), whereas **1b** is depicted as a blue CPK representation. b) Hydrogen-bonding interactions between **1b** and the His438 and Trp396 residues.



PDI reduces the insulin disulfide bonds in the presence of dithiothreitol (DTT), and then the aggregation of the reduced insulin chains is measured at 620 nm. PDI activity was clearly impaired in the presence of *pAC 1b* in a concentration-dependent fashion (see Figure S17), thus indicating an important role of the interaction between the calixarene scaffold and PDI in determining the chaperone inactivation.<sup>[6]</sup>

Next, we evaluated the *in vitro* ability of *pAC 1b* to inhibit the viability and the metabolic activity of cancer cells. Thus, two different human tumor cell lines were cultured: CAL-27 (oral adenocarcinoma cell line) and PC-3 (human prostate cancer cell line). A clear stock solution of the *pAC* derivative **1b** in dimethyl sulfoxide was prepared and used for the addition of **1b** to the cell culture medium. After incubation with compound **1b** for 24 h, the cell viability was evaluated by a trypan blue exclusion test and the metabolic activity through a 3-(4,5-dimethylthiazol-2-yl)-2,5-diphenyl-tetrazolium bromide (MTS) reduction assay, which measures the ability of a mitochondrial dehydrogenase enzyme from viable cells to cleave the tetrazolium rings. As a positive control, cells were treated with a known chemotherapeutic drug, 7-ethyl-10-hydroxycamptothecin (SN38), an active metabolite of irinotecan, and the known PDI inhibitor 16F16,<sup>[21]</sup> at concentrations of 0.35, 0.75, 1.5, 3.6, and 12  $\mu\text{M}$ .<sup>[22]</sup> The results are expressed in Table 1 as  $\text{IC}_{50}$  values

**Table 1:** Evaluation of the cytotoxicity of *pAC 1b* in comparison with that of SN38 and the known PDI inhibitor 16F16.

	Cell line	$\text{IC}_{50} \pm \text{SD} [\mu\text{M}]^{\text{a}}$	$\text{CC}_{50} \pm \text{SD} [\mu\text{M}]^{\text{b}}$
<b>1b</b>	CAL-27	$20.5 \pm 0.8$	$31.0 \pm 4$
<b>1b</b>	PC-3	$24.5 \pm 0.9$	$283 \pm 10$
SN38	CAL-27	$3.0 \pm 0.9$	$3.2 \pm 0.3$
SN38	PC-3	$11.5 \pm 0.2$	$6.9 \pm 0.9$
16F16	CAL-27	$7.6 \pm 0.4$	$8.8 \pm 1.9$
16F16	PC-3	$25.0 \pm 0.6$	$14.7 \pm 1.6$

[a]  $\text{IC}_{50}$  is the concentration required to inhibit 50% of cell viability.

[b]  $\text{CC}_{50}$  is the concentration required to inhibit the metabolic activity of 50% of the cells, as evaluated in the CAL-27 and PC-3 cell lines by a MTS assay.

for the viability assay and  $\text{CC}_{50}$  values for the metabolic assay (these values are the concentration of the compound at which 50% of cells are viable or metabolically active).

The *pAC* derivative **1b** was cytotoxic toward CAL-27 and PC-3 cell lines with  $\text{IC}_{50}$  values of  $(20.5 \pm 0.8)$  and  $(24.5 \pm 0.9) \mu\text{M}$ , respectively, and SN38 showed cytotoxicity toward CAL-27 and PC-3 with  $\text{IC}_{50}$  values of  $(3.0 \pm 0.9)$  and  $(11.5 \pm 0.2) \mu\text{M}$ , respectively. Interestingly, **1b** inhibited PC-3 proliferation with an  $\text{IC}_{50}$  value that overlapped with that of the commercial 16F16<sup>[21]</sup> PDI inhibitor, thus suggesting a similar action mode. Regarding the effect of **1b** on the metabolic activity of CAL-27 and PC-3 cells, we found  $\text{CC}_{50}$  values of  $(31 \pm 0.3)$  and  $(283 \pm 10) \mu\text{M}$ , respectively, which are higher than those shown by both SN38 and 16F16 ( $3.2$ – $14.7 \mu\text{M}$ ). These data demonstrated that *pAC 1b* exhibits biological activity toward tumor cells that is comparable to that of both SN38 and 16F16. Notably, the two cell lines were equally susceptible to the cytotoxic effect of *pAC 1b*, whereas PC-3

was more resistant than CAL-27 to its metabolic inhibitory effect, as shown by the  $\text{CC}_{50}$  value of  $(283 \pm 10) \mu\text{M}$ . The metabolic inhibitory effect might depend on the sensitivity of the specific cell line itself and might indicate a preferential cytostatic effect owing to inhibition of the metabolic activity of CAL-27. However, *pAC 1b* seems to be equally cytotoxic and able to metabolically inhibit CAL-27, as it showed  $\text{IC}_{50}$  and  $\text{CC}_{50}$  values that were 7- and 10-fold higher than those exhibited by SN38, respectively. Interestingly, **1b** inhibited PC-3 proliferation with a  $\text{CC}_{50}$  value around 20 times higher than that of the 16F16 inhibitor. Conversely, the  $\text{IC}_{50}$  and  $\text{CC}_{50}$  values of **1b** toward CAL-27 were both around three times higher than those of the 16F16 inhibitor. Taken together, these results indicate that the *in vitro* biological activity of *pAC 1b* toward tumor cell lines is only slightly lower than that of a known chemotherapeutic drug and that of a genuine PDI inhibitor, and they encourage the development of further assays to test the activity of *pAC 1b* against a broader range of tumor cell lines.

In conclusion, we have introduced herein MS-based chemical-proteomics technology as a third general strategy to study the biomolecular-recognition properties of given calixarene derivatives. In particular, we have shown that simply designed calix[4]arene derivatives bearing acetamido groups at the *exo* rim (*pAC*) were able to recognize the protein disulfide isomerase (PDI), which was fished from a crude extract of HeLa cells. Western blot and surface plasmon resonance (SPR) studies indicated a direct interaction between PDI protein and the *pAC* derivative. Increased PDI levels have been documented previously in a variety of human cancers, thus suggesting that PDI is a promising druggable target. Biological *in vitro* tests showed that *pAC* derivative **1b** was able to inhibit the PDI chaperone activity: cytotoxic and cytostatic activity toward CAL-27 and PC-3 was observed. Finally, docking studies showed that both hydrogen-bonding and hydrophobic interactions seem to be the main driving forces for the stabilization of the PDI/*pAC* complexes, in agreement with observations made during the formation of natural complexes between PDI enzymes and misfolded protein substrates.

## Acknowledgements

We thank the Italian MIUR (PRIN 20109Z2XRJ\_006 and 20109Z2XRJ\_005) for financial support, CAPES (Brasil) for financial support to A.L.D.A. (scholarship contract no. 14952/13-0), and the CETIS (PONA3\_00138), Università di Salerno, for 600 MHz NMR instrument time.

**Keywords:** biomolecular recognition · calixarenes · chemical proteomics · proteins · surface plasmon resonance

**How to cite:** *Angew. Chem. Int. Ed.* **2015**, *54*, 15405–15409  
*Angew. Chem.* **2015**, *127*, 15625–15629

- [1] a) H. S. Park, Q. Lin, A. D. Hamilton, *J. Am. Chem. Soc.* **1999**, *121*, 8–13; b) M. W. Pecuh, A. D. Hamilton, *Chem. Rev.* **2000**, *100*, 2479–2493; c) M. A. Blaskovich, Q. Lin, F. L. Delarue, J.

- Sun, H. S. Park, D. Coppola, A. D. Hamilton, S. M. Sebt, *Nat. Biotechnol.* **2000**, *18*, 1065–1070; d) H. S. Park, Q. Lin, A. D. Hamilton, *Proc. Natl. Acad. Sci. USA* **2002**, *99*, 5105–5109; e) L. Baldini, A. Casnati, F. Sansone, R. Ungaro, *Chem. Soc. Rev.* **2007**, *36*, 254–266; f) A. Casnati, F. Sansone, R. Ungaro, *Acc. Chem. Res.* **2003**, *36*, 246–254; g) S. Cherenok, A. Vovk, I. Muravyova, A. Shivanyuk, V. Kukhar, J. Lipkowski, V. Kalchenko, *Org. Lett.* **2006**, *8*, 549–552; h) M. G. Chini, S. Terracciano, R. Riccio, G. Bifulco, R. Ciao, C. Gaeta, F. Troisi, P. Neri, *Org. Lett.* **2010**, *12*, 5382–5385; i) S. Francese, A. Cozzolino, L. Caputo, C. Esposito, M. Martino, C. Gaeta, F. Troisi, P. Neri, *Tetrahedron Lett.* **2005**, *46*, 1611–1615; j) T. Mecca, G. M. L. Consoli, C. Geraci, F. Cunsolo, *Bioorg. Med. Chem.* **2004**, *12*, 5057–5062; k) S. Gordo, V. Martos, E. Santos, M. Menendez, C. Bo, E. Giralt, J. de Mendoza, *Proc. Natl. Acad. Sci. USA* **2008**, *105*, 16426–16431; l) S. N. Gradl, J. P. Felix, E. Y. Isacoff, M. L. Garcia, D. Trauner, *J. Am. Chem. Soc.* **2003**, *125*, 12668–12669; m) V. Martos, S. C. Bell, E. Santos, E. Y. Isacoff, D. Trauner, J. de Mendoza, *Proc. Natl. Acad. Sci. USA* **2009**, *106*, 10482–10486; n) T. Schrader, *Nat. Chem.* **2012**, *4*, 519–520; o) R. Zadnarm, N. S. Alavijeh, *RSC Adv.* **2014**, *4*, 41529–41542.
- [2] a) K. Wang, D. S. Guo, H. Q. Zhang, D. Li, X. L. Zheng, Y. Liu, *J. Med. Chem.* **2009**, *52*, 6402–6412; b) A. W. Coleman, S. Jebors, S. Cecillon, P. Perret, D. Garin, D. Marti-Battle, M. Moulin, *New J. Chem.* **2008**, *32*, 780–782.
- [3] a) U. Rix, G. Superti-Furga, *Nat. Chem. Biol.* **2005**, *1*, 616–624; b) L. Margarucci, M. C. Monti, A. Tosco, R. Riccio, A. Casapullo, *Angew. Chem. Int. Ed.* **2010**, *49*, 3960–3963; *Angew. Chem.* **2010**, *122*, 4052–4055; c) L. Margarucci, M. C. Monti, C. Cassiano, M. Mozzicafreddo, M. Angeletti, R. Riccio, A. Tosco, A. Casapullo, *Chem. Commun.* **2013**, *49*, 5844–5846; d) L. Margarucci, M. C. Monti, A. Mencarelli, C. Cassiano, S. Fiorucci, R. Riccio, A. Zampella, A. Casapullo, *Mol. Biosyst.* **2012**, *8*, 1412–1417; e) C. Cassiano, M. C. Monti, C. Festa, A. Zampella, R. Riccio, A. Casapullo, *ChemBioChem* **2012**, *13*, 1953–1958; f) A. Doerr, *Nat. Methods* **2010**, *7*, 34–34; g) M. Bantscheff, A. Scholten, A. J. R. Heck, *Drug Discovery Today* **2009**, *14*, 1021–1029.
- [4] For representative reports on the supramolecular abilities of calixarene derivatives functionalized at the *exo* rim with amide groups, see: a) M. H. Lee, Q.-Y. Cao, S. K. Kim, J. L. Sessler, J. S. Kim, *J. Org. Chem.* **2011**, *76*, 870–874; b) F. Troisi, C. Gaeta, T. Pierro, P. Neri, *Tetrahedron Lett.* **2009**, *50*, 5113–5115; c) R. E. Brewster, S. B. Shuker, *J. Am. Chem. Soc.* **2002**, *124*, 7902–7903; d) M. S. Becherer, B. Schade, C. Böttcher, A. Hirsch, *Chem. Eur. J.* **2009**, *15*, 1637–1648; e) F. Troisi, A. Russo, C. Gaeta, G. Bifulco, P. Neri, *Tetrahedron Lett.* **2007**, *48*, 7986–7989.
- [5] C. Cassiano, L. Margarucci, R. Esposito, R. Riccio, A. Tosco, A. Casapullo, M. C. Monti, *Chem. Commun.* **2014**, *50*, 6043–6045.
- [6] See Supporting Information for further details.
- [7] As known from previous pulldown studies (Refs. [3,5]) and in accordance with the multitarget concept (Refs. [3a,g]), other potential partners for *p*-AC **1a** cannot be excluded by the fishing procedure (see Table S4 and Figure S8). However, on the basis of the individual scores, they can be considered as less likely candidates. The possible biological significance of the other potential targets will be investigated in future studies.
- [8] R. F. Goldberger, C. J. Epstein, C. B. Anfinsen, *J. Biol. Chem.* **1964**, *239*, 1406–1410.
- [9] B. Wilkinson, H. F. Gilbert, *Biochim. Biophys. Acta Proteins Proteomics* **2004**, *1699*, 35–44.
- [10] a) P. E. Lovat, M. Corazzari, J. L. Armstrong, *Cancer Res.* **2008**, *68*, 5363–5369; b) R. B. Freedman, *Cell* **1989**, *57*, 1069–1072; c) A. R. Frand, J. W. Cuzzo, C. A. Kaiser, *Trends Cell Biol.* **2000**, *10*, 203–210.
- [11] C. W. Gruber, M. Cemazar, B. Heras, J. L. Martin, D. J. Craik, *Trends Biochem. Sci.* **2006**, *31*, 455–464.
- [12] T. Bonome, D. A. Levine, J. Shih, M. Randonovich, C. A. Pise-Masison, F. Bogomolny, L. Ozbun, J. Brady, J. C. Barrett, J. Boyd, M. J. Birrer, *Cancer Res.* **2008**, *68*, 5478–5486.
- [13] J. B. Welsh, L. M. Sapinoso, A. I. Su, S. G. Kern, J. Wang-Rodriguez, C. A. Moskaluk, H. F. Frierson, Jr., G. M. Hampton, *Cancer Res.* **2001**, *61*, 5974–5978.
- [14] D. G. Beer, S. L. Kardia, C. C. Huang, T. J. Giordano, A. M. Levin, D. E. Misek, L. Lin, G. Chen, T. G. Gharib, D. G. Thomas, M. L. Lizyness, R. Kuick, S. Hayasaka, J. M. Taylor, M. D. Iannettoni, M. B. Orringer, S. Hanash, *Nat. Med.* **2002**, *8*, 816–824.
- [15] K. Basso, A. A. Margolin, G. Stolovitzky, U. Klein, R. Dalla-Favera, A. Califano, *Nat. Genet.* **2005**, *37*, 382–390.
- [16] D. S. Rickman, M. P. Bobek, D. E. Misek, R. Kuick, M. Blaivas, D. M. Kurnit, J. Taylor, S. M. Hanash, *Cancer Res.* **2001**, *61*, 6885–6891.
- [17] S. Haeffliger, C. Klebig, K. Schaubitzer, J. Schardt, N. Timchenko, B. U. Mueller, T. Pabst, *Blood* **2011**, *117*, 5931–5940.
- [18] a) G. Tian, S. Xiang, R. Noiva, W. J. Lennarz, H. Schindelin, *Cell* **2006**, *124*, 61–73; b) C. Wang, W. Li, J. Ren, J. Fang, H. Ke, W. Gong, W. Feng, C. C. Wang, *Antioxid. Redox Signaling* **2013**, *19*, 36–45.
- [19] C. Wang, J. Yu, L. Huo, L. Wang, W. Feng, C. C. Wang, *J. Biol. Chem.* **2012**, *287*, 1139–1149.
- [20] a) R. Jasuja, F. H. Passam, D. R. Kennedy, S. H. Kim, L. van Hessem, L. Lin, S. R. Bowley, S. S. Joshi, J. F. Dilks, B. Furie, B. C. Furie, R. J. Flaumenhaft, *J. Clin. Invest.* **2012**, *122*, 2104–2113; b) A. M. Smith, J. Chan, D. Oksenberg, R. Urfer, D. S. Wexler, A. Ow, L. Gao, A. McAlorum, S.-G. Huang, *J. Biomol. Screening* **2004**, *9*, 614–620.
- [21] 16F16 is a commercial synthetic PDI inhibitor that prevents apoptosis induced by mutant huntingtin protein; see: B. G. Hoffstrom, A. Kaplan, R. Letso, R. S. Schmid, G. J. Turmel, D. C. Lo, B. R. Stockwell, *Nat. Chem. Biol.* **2010**, *6*, 900–906.
- [22] A. Minutolo, S. Grelli, F. Marino-Merlo, F. M. Cordero, A. Brandi, B. Macchi, A. Mastino, *Cell Death Dis.* **2012**, *3*, 1–9.

Received: September 15, 2015

Published online: October 29, 2015